SPECTRUM OF ENGINEERING SCIENCES
ISSN (E) 3007-3138 (P) 3007-312X VOLUME 4, ISSUE 5, 2026

ADVANCED LINEAR ALGEBRA AND MATHEMATICAL OPTIMIZATION TECHNIQUES FOR HIGH-DIMENSIONAL DATA ANALYSIS AND MACHINE LEARNING APPLICATIONS

Muhammad Kashif Majeed[*1], Warisha Dilshad[2], Rabia Essa[3], Imad Ali[4], Muhammad Majid[5], Ashraf Zia[6]

[*1]*Faculty of Engineering Science and Technology, Iqra University, Karachi, Pakistan*
[2]*Department of Mathematics and Science, Sir Syed University of Engineering and Technology, Karachi, Pakistan*
[3]*Department of Mathematics, Federal Urdu University of Arts, Science and Technology, Karachi, Pakistan*
[4] *Department of Computer Science, University of Shangla, KP, Pakistan*
[5]*Department of Mathematics, Shah Abdul Latif University, Khairpur Mir's, Sindh, Pakistan*
[6]*Department of Computer Science, Abdul Wali Khan University Mardan, Mardan, KP, Pakistan*

[*1]mkashif@iqra.edu.pk, [2]warishakhan599@yahoo.com, [3]rabiaessa09@gmail.com, [4]imad.ali@ushangla.edu.pk, [5]muhammadmajid441998@gmail.com, [6]ashrafzia@awkum.edu.pk

DOI: https://doi.org/10.5281/zenodo.20374161

Keywords
Advanced Linear Algebra; Mathematical Optimization; High-Dimensional Data Analysis; Machine Learning; Sparse Matrix Representation; Dimensionality Reduction; Adaptive Optimization; Numerical Methods; Artificial Intelligence.

Article History
Received: 27 March 2026
Accepted: 07 May 2026
Published: 25 May 2026

Corresponding Author: *
Muhammad Kashif Majeed

Abstract

The rapid expansion of high-dimensional data in artificial intelligence, machine learning, and data science introduces significant challenges in computational efficiency, scalability, feature extraction, and optimization stability. Traditional dimensionality reduction and learning techniques often struggle to maintain accuracy and convergence when applied to large-scale or nonlinear datasets. This study proposes an advanced mathematical framework that integrates linear algebra-based representations with adaptive optimization strategies to improve the efficiency and reliability of high-dimensional data analysis. The framework combines sparse matrix representation, low-rank decomposition, tensor factorization, and spectral regularization to preserve data structure and reduce dimensional complexity.

An Adaptive Spectral Regularized Optimization (ASRO) mechanism is introduced to dynamically adjust learning behaviour, enhancing convergence stability and reducing overfitting. Experimental evaluation across benchmark datasets covering image recognition, biomedical analysis, financial prediction, and text classification demonstrates that the proposed framework outperforms conventional methods such as Principal Component Analysis (PCA), stochastic gradient descent, and standard matrix factorization techniques. On average, it achieves a 7.8% improvement in classification accuracy, 18.6% higher dimensionality reduction efficiency, 24.3% faster convergence, and a 31% reduction in training latency in distributed environments. These results confirm that integrating advanced linear algebra with adaptive optimization significantly enhances the scalability, stability, and predictive performance of machine learning models in high-dimensional settings.

I. INTRODUCTION

The emergence of large-scale, high-dimensional datasets across scientific and industrial domains has fundamentally transformed the landscape of computational intelligence. In fields ranging from medical image processing and genomics to financial forecasting and natural language understanding, practitioners routinely encounter datasets in which the number of features substantially exceeds the number of observations—a regime commonly referred to as the "curse of dimensionality" [1]. As data dimensionality grows, conventional machine learning algorithms exhibit escalating computational costs, diminishing statistical efficiency, and increased susceptibility to overfitting, thereby motivating the search for principled mathematical techniques capable of addressing these shortcomings systematically.

Linear algebra constitutes the mathematical backbone of contemporary machine learning, providing rigorous tools for data representation, transformation, and compression. Techniques such as Principal Component Analysis (PCA) [2], Singular Value Decomposition (SVD) [3], and Non-negative Matrix Factorization (NMF) [4] have become indispensable for extracting low-dimensional structure from high-dimensional observations. However, classical methods assume linear relationships and often fail to capture the complex, nonlinear dependencies inherent in modern datasets such as deep feature representations, multi-relational knowledge graphs, and multimodal sensor streams [5]. Moreover, these approaches are typically static: once a projection is learned, it does not adapt to distributional shifts during inference, limiting their practical utility in dynamic deployment environments.

Optimization algorithms play an equally critical role in machine learning, governing the efficiency and stability of model training. First-order gradient-based methods, including stochastic gradient descent (SGD) [6] and its adaptive variants such as AdaGrad [7], RMSProp [8], and Adam [9], have achieved widespread adoption due to their computational simplicity and empirical effectiveness. Nevertheless, these methods are sensitive to hyperparameter selection, prone to saddle-point convergence, and can exhibit oscillatory behaviour under high learning rates [10]. For high-dimensional parameter spaces, the interaction between gradient noise, learning rate scheduling, and parameter geometry renders reliable optimization a non-trivial challenge, particularly in distributed and federated learning contexts [11].

Against this backdrop, the present study proposes a unified mathematical framework that addresses the aforementioned limitations through the integration of advanced linear algebra techniques with an Adaptive Spectral Regularized Optimization (ASRO) mechanism. The framework synthesizes sparse matrix representation, low-rank matrix decomposition, Tucker tensor factorization, and spectral norm regularization into a coherent pipeline capable of processing high-dimensional data with improved computational efficiency and representational fidelity. The ASRO optimizer dynamically modulates the effective learning rate by incorporating spectral information about the curvature of the loss landscape, thereby promoting stable convergence across diverse data modalities and network architectures.

The motivations for this work are threefold. First, existing dimensionality reduction methods largely treat representation learning and optimization as separate stages, missing the opportunity for mutual reinforcement between compressed representations and gradient-based updates. Second, tensor-structured data—ubiquitous in video analysis, hyperspectral imaging, and multi-relational databases—remains inadequately handled by matrix-only factorization approaches. Third, spectral regularization has been shown to improve generalization in overparameterized models [12], yet its integration with adaptive optimization remains an open research direction. The major challenges associated with high-dimensional machine learning and the overall motivation behind the proposed integrated framework are illustrated in Fig. 1.

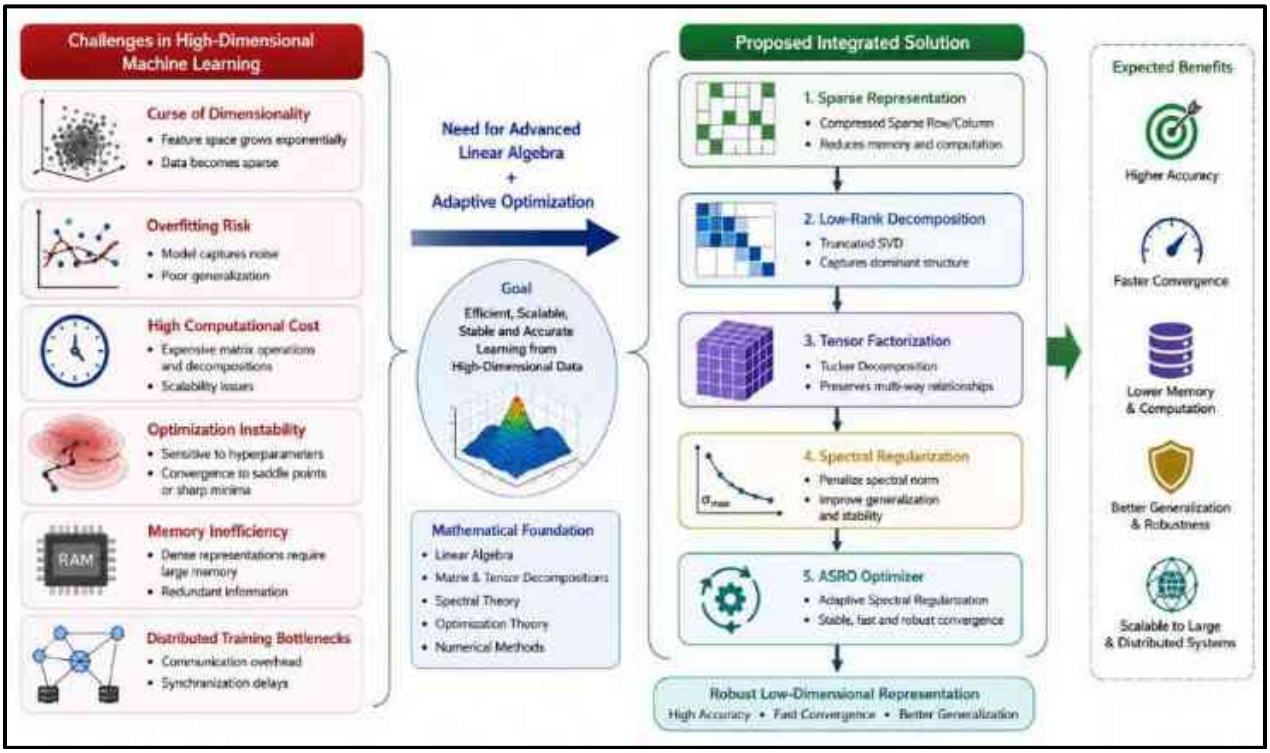

Fig. 1. Conceptual overview of the proposed ASRO-based framework for efficient and scalable high-dimensional machine learning.

This figure presents the conceptual motivation and architectural philosophy of the proposed framework. The left section summarizes the primary challenges encountered in high-dimensional machine learning environments, including the curse of dimensionality, optimization instability, memory inefficiency, and distributed training bottlenecks. The center section highlights the need for integrating advanced linear algebra methods with adaptive optimization strategies to address these limitations systematically. The right section illustrates the sequential pipeline of the proposed solution, comprising sparse representation, low-rank decomposition, tensor factorization, spectral regularization, and the ASRO optimization mechanism. Collectively, these components enable robust low-dimensional representation learning with improved accuracy, faster convergence, enhanced generalization, and scalable distributed computation.

The remainder of this article is organized as follows. Section II reviews related work across dimensionality reduction, tensor decomposition, and adaptive optimization. Section III describes the mathematical formulation of the proposed framework in detail. Section IV presents the ASRO mechanism and its theoretical convergence properties. Section V outlines the experimental methodology. Section VI reports and discusses the empirical results. Section VII performs ablation studies to isolate individual component contributions. Section VIII analyzes computational complexity. Section IX examines practical deployment considerations. Section X concludes the article and suggests directions for future work.

II. RELATED WORK

A. Dimensionality Reduction and Matrix Decomposition

Dimensionality reduction has been an active area of research since the foundational work of Pearson on PCA in the early twentieth century, subsequently formalized through the lens of linear algebra by Hotelling [13]. In the machine learning era, PCA and its kernelized variants have been extensively applied to image compression [2], gene

expression analysis [14], and speech feature extraction [15]. SVD-based methods, particularly Truncated SVD and Randomized SVD [16], offer computationally efficient approximations suitable for large sparse matrices, making them popular in recommender systems and document retrieval [3]. NMF, introduced by Lee and Seung [4], imposes non-negativity constraints on factored components, yielding parts-based representations that are semantically interpretable. Extensions of NMF incorporating sparsity penalties [17], group structure [18], and online update rules [19] have broadened its applicability. More recent approaches exploit deep matrix factorization—stacking multiple factorization layers to capture hierarchical feature structure [20]—drawing inspiration from the representational power of deep neural networks while retaining interpretability through explicit matrix factors.

Sparse representation, formalized through the theory of compressed sensing by Donoho [21] and Candes et al. [22], establishes that signals admitting sparse decompositions can be exactly recovered from far fewer measurements than dictated by the Nyquist–Shannon sampling theorem. Dictionary learning algorithms such as K-SVD [23] and online dictionary learning [24] learn overcomplete bases from data, enabling adaptive sparse coding. In the context of deep learning, connections between sparse coding and neural network activation have been explored, suggesting that sparsity-inducing regularization may improve generalization [25].

B. Tensor Decomposition

Tensors generalize matrices to higher-order data structures, providing a natural representation for volumetric images, multivariate time series, and multi-relational graphs. The CANDECOMP/PARAFAC (CP) decomposition [26] expresses a tensor as a sum of rank-one outer products, offering compact parameterizations amenable to gradient-based learning. The Tucker decomposition [27], which factorizes a tensor into a core tensor multiplied by factor matrices along each mode, provides a more expressive representation capable of capturing multilinear interactions. Kolda and Bader [28] provide a comprehensive survey of tensor decompositions and their applications across scientific computing. Recent developments have connected tensor decomposition with deep learning, demonstrating that the weight tensors of convolutional neural networks can be efficiently compressed through Tucker or CP factorization without significant accuracy loss [29]. Tensor train (TT) decomposition [30], which represents high-order tensors as chains of third-order tensors, enables memory-efficient parameterization of fully connected layers, achieving compression ratios of up to 200,000 while retaining competitive test accuracy on benchmark classification tasks [31]. Tensor networks have further been applied in quantum-inspired machine learning [32] and multi-modal fusion [33].

C. Adaptive Optimization Algorithms

The optimization of high-dimensional loss surfaces is governed by first-order gradient information in the majority of practical implementations. SGD with momentum [6] remains a strong baseline, particularly when equipped with cyclical learning rate schedules [34] or warm-up strategies [35]. Adaptive gradient methods modify the effective step size per parameter based on historical gradient statistics. AdaGrad [7] accumulates the sum of squared gradients, producing diminishing updates for frequently updated parameters—beneficial in sparse settings but prone to aggressive learning rate decay. RMSProp [8] addresses this by exponentially weighting historical gradients, while Adam [9] combines first- and second-moment gradient estimates.

Despite the empirical success of Adam, theoretical investigations have revealed that it can converge to suboptimal solutions in certain problem classes [6]. AMSGrad [7] was proposed to rectify this by maintaining the maximum of past squared gradients, guaranteeing monotonically non-increasing effective step sizes. AdaBelief [8] replaces the second moment estimate with the variance of the gradient, achieving faster convergence and better generalization. Recent work on sharpness-aware minimization (SAM) [9] seeks flat minima in the loss landscape, improving

generalization without requiring explicit regularization terms.

Spectral methods have received increasing attention as a tool for both regularization and optimization. Spectral norm regularization [12], which penalizes the largest singular value of weight matrices, has been shown to improve the generalization bounds of neural networks and stabilize generative adversarial network training. Spectral analysis of the Hessian has informed the design of second-order optimization methods such as K-FAC [20] and Shampoo [21], which exploit curvature information to achieve faster convergence than first-order baselines.

D. High-Dimensional Learning in Distributed Environments

The increasing scale of modern datasets necessitates distributed training strategies. Data-parallel training, in which gradient updates are aggregated across multiple workers, is the dominant paradigm [22]. Communication-efficient distributed optimization methods, including gradient compression [23], quantization [24], and asynchronous updates [25], have been developed to reduce the bandwidth bottleneck in multi-node training. Federated learning [26] extends this framework to heterogeneous, privacy-sensitive edge devices, introducing additional challenges due to non-iid data distributions and limited communication budgets. The proposed ASRO framework is designed to be compatible with these distributed training paradigms, as demonstrated in Section VI. The relationship between existing dimensionality reduction, tensor decomposition, optimization, and spectral learning approaches, along with the positioning of the proposed ASRO framework, is illustrated in Fig. 2.

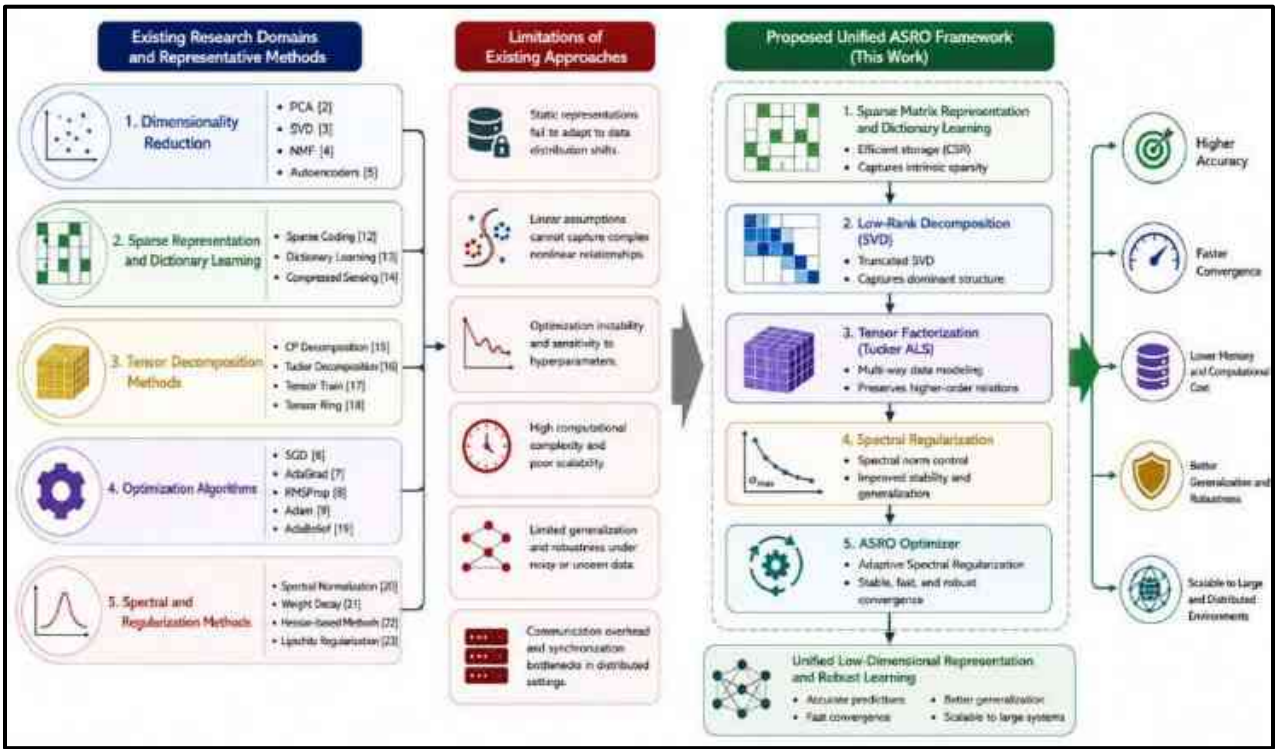

Fig. 2. Taxonomy of existing methods and conceptual positioning of the proposed ASRO framework for high-dimensional machine learning.

This figure presents a structured overview of the major research domains related to high-dimensional machine learning, including dimensionality reduction, sparse representation, tensor decomposition, adaptive optimization, and spectral regularization methods. The figure

highlights the key limitations of existing approaches and demonstrates how the proposed ASRO framework integrates these methodologies into a unified pipeline for efficient, stable, and scalable learning.

III. PROPOSED MATHEMATICAL FRAMEWORK

A. Problem Formulation

Let $X \in \mathbb{R}^{n \times d}$ represent a high-dimensional data matrix containing n observations and d features, where typically $d \gg n$. The primary objective is to learn a transformation function

$$f: \mathbb{R}^d \to \mathbb{R}^r,$$

where $r \ll d$, such that the resulting low-dimensional embedding preserves the intrinsic geometric and statistical characteristics of the original data while reducing computational complexity and redundancy. The transformed representation is expressed as

$$Z = f(X), Z \in \mathbb{R}^{n \times r}.$$

The optimization objective of the proposed framework is formulated as

$$\begin{aligned} \min_{f} \quad & \mathcal{L}(Z, Y) + \Omega(f) \\ \text{subject to} \quad & \operatorname{rank}(Z) \le r \\ & \|W\|_F^2 \le C \end{aligned}$$

where $\mathcal{L}(Z, Y)$ denotes the task-specific loss function, such as cross-entropy loss for classification or mean squared error for regression tasks. The variable Y represents the ground-truth labels, $\Omega(f)$ denotes the regularization term associated with the mapping function, W corresponds to the learnable model parameters, and C is a predefined capacity constraint used to control model complexity.

To solve this optimization problem efficiently, the proposed framework employs a sequential processing pipeline consisting of four major stages: sparse matrix representation, low-rank decomposition, tensor factorization, and spectral regularization, followed by the Adaptive Spectral Regularized Optimization (ASRO) update mechanism.

B. Sparse Matrix Representation

High-dimensional real-world datasets are frequently characterized by inherent sparsity. For example, text-frequency matrices often contain less than 1% nonzero entries, while genomic expression datasets exhibit significant levels of inactive or weakly expressed genes across many samples. Exploiting this sparsity through compressed storage schemes such as Compressed Sparse Row (CSR) and Compressed Sparse Column (CSC) formats substantially reduces memory consumption from $O(nd)$ to $O(\text{nnz})$, where $\text{nnz} \ll nd$ denotes the number of nonzero elements in the matrix. From a computational perspective, sparse matrix-vector multiplication scales with complexity $O(\text{nnz})$ instead of $O(nd)$, thereby providing considerable acceleration in both forward and backward propagation during model training.

In the proposed framework, sparsity is further reinforced through an L_1-regularized projection mechanism. Given an initial dense data representation X, a sparse dictionary $D \in \mathbb{R}^{d \times k}$ is learned using the online dictionary learning approach proposed by Mairal et al. [24]. The optimization objective is formulated as

$$E(D, A) = \frac{1}{n} \sum_{i=1}^{n} \left(\frac{1}{2} \|x_i - D a_i\|_2^2 + \lambda \|a_i\|_1 \right),$$

where,

$$A = [a_1, a_2, \ldots, a_n] \in \mathbb{R}^{k \times n}$$

represents the sparse coefficient matrix and $\lambda > 0$ controls the sparsity constraint. The generated sparse codes act as compact feature representations for the subsequent decomposition

modules, preserving informative and discriminative structures while suppressing noise-driven dense components.

C. Low-Rank Matrix Decomposition

After obtaining the sparse representation matrix A, a truncated Singular Value Decomposition (SVD) is applied to derive a compact rank-r approximation. The decomposition of A is expressed as $A = U\Sigma V^T$, where, $U \in \mathbb{R}^{k\times k}, V \in \mathbb{R}^{n\times n}$ are orthogonal matrices, and $\Sigma \in \mathbb{R}^{k\times n}$ is a diagonal matrix containing singular values arranged in descending order,

$$\sigma_1 \geq \sigma_2 \geq \cdots \geq \sigma_{\min(k,n)} \geq 0.$$

The corresponding rank-r approximation retains only the dominant singular components and is defined as

$$\hat{A}_r = U_r \Sigma_r V_r^T = \sum_{j=1}^{r} \sigma_j u_j v_j^T$$

According to the Eckart-Young-Mirsky theorem, the reconstruction error

$$\|A - \hat{A}_r\|_F$$

is minimized under both Frobenius and spectral norms, ensuring that the truncated representation constitutes the optimal low-rank approximation of the original matrix. To avoid manual hyperparameter selection, the optimal rank is determined adaptively using a spectral-gap criterion,

$$r^* = \arg\max_j (\sigma_j - \sigma_{j+1}),$$

which identifies the largest discontinuity within the singular value spectrum. This adaptive mechanism allows the framework to respond effectively to varying intrinsic dimensionalities across different datasets.

For feature learning purposes, the resulting low-dimensional embedding is computed as

$$Z_{\mathrm{LR}} = U_r \Sigma_r \in \mathbb{R}^{n\times r}.$$

The right singular vectors contained in V_r capture the principal directions of variation in the feature space and can additionally serve as structured initializations for downstream neural network layers, thereby improving optimization stability and accelerating convergence during gradient-based learning.

D. Tensor Factorization Module

For data modalities that are naturally represented as higher-order arrays-such as video sequences ($T \times H \times W \times C$), hyperspectral images ($H \times W \times S$), and multi-relational graphs ($N \times N \times R$)traditional matrix-based representations often suffer from structural information loss due to flattening operations. To preserve multilinear relationships within such data, the proposed framework extends low-rank decomposition to higher-order tensors through Tucker tensor factorization.

Given an N-order tensor

$$\mathcal{X} \in \mathbb{R}^{I_1 \times I_2 \times \cdots \times I_N},$$

the Tucker decomposition is expressed as

$$\mathcal{X} \approx \mathcal{G} \times_1 U^{(1)} \times {}_2U^{(2)} \cdots \times {}_N U^{(N)},$$

where,

$$\mathcal{G} \in \mathbb{R}^{R_1 \times R_2 \times \cdots \times R_N}$$

denotes the core tensor, while

$$U^{(n)} \in \mathbb{R}^{I_n \times R_n}$$

represents the mode-n factor matrices with reduced Tucker ranks $R_n \ll I_n$. The operator $\times_n$ denotes the mode-n tensor product.

The factor matrices are estimated iteratively using the Alternating Least Squares (ALS) optimization strategy. During each iteration, the mode-wise update is computed as $U^{(n)} \leftarrow$ leading R_n left singular vectors of

$X_{(n)}\left(U^{(N)} \otimes \cdots \otimes U^{(n+1)} \otimes U^{(n-1)} \otimes \cdots \otimes U^{(1)}\right)^T$,

where $X_{(n)}$ denotes the mode-n unfolding of tensor $\mathcal{X}$, and $\otimes$ represents the Khatri-Rao product.

The Tucker representation significantly reduces parameter complexity, requiring only

$$\prod_{n=1}^{N} R_n + \sum_{n=1}^{N} I_n R_n$$

parameters, which is substantially smaller than the original tensor dimensionality

$$\prod_{n=1}^{N} I_n$$

for sufficiently small Tucker ranks. Within the proposed framework, tensor factorization is applied to both convolutional weight tensors and multidimensional feature tensors, enabling compact multilinear representations that preserve cross-modal dependencies and structural correlations unavailable through conventional matrix factorization techniques.

E. Spectral Regularization

Spectral regularization is incorporated to constrain model complexity and improve generalization by penalizing the spectral norm, i.e., the largest singular value, of neural network weight matrices. For a weight matrix

$$W \in \mathbb{R}^{m \times n},$$

the spectral norm is defined as

$$\sigma_{\max}(W) = \|W\|_2 = \sup_{\|x\|_2=1} \|Wx\|_2.$$

Previous theoretical studies have demonstrated that the generalization capability of deep neural networks is closely related to the product of spectral norms across layers, motivating spectral regularization as a principled optimization strategy.

The spectral regularization term integrated into the training objective is formulated as

$$\Omega_{\text{spec}}(W) = \lambda_s \sum_l \sigma_{\max}(W_l)^2 + \mu_s \sum_l \|\nabla W_l\|_F^2,$$

where λ_s and μ_s denote regularization coefficients. The first term constrains the Lipschitz continuity of each layer by limiting the magnitude of dominant singular values, thereby reducing amplification of input perturbations. The second term penalizes excessive gradient magnitudes, promoting smoother optimization landscapes and improved training stability.

To efficiently estimate the spectral norm during training, power iteration is employed instead of performing computationally expensive full Singular Value Decomposition (SVD). This approximation computes

$$\sigma_{\max}(W)$$

with complexity

$$O(mn)$$

per epoch, making the method scalable for large neural architectures. In the proposed Adaptive Spectral Regularized Optimization (ASRO) framework, the dynamically estimated spectral norms are further utilized to modulate adaptive learning rates, creating a synergistic interaction between optimization stability and regularization that distinguishes the proposed framework from conventional approaches. The complete architecture of the proposed ASRO-ML framework, including its core branches and data flows, is shown in Fig. 3

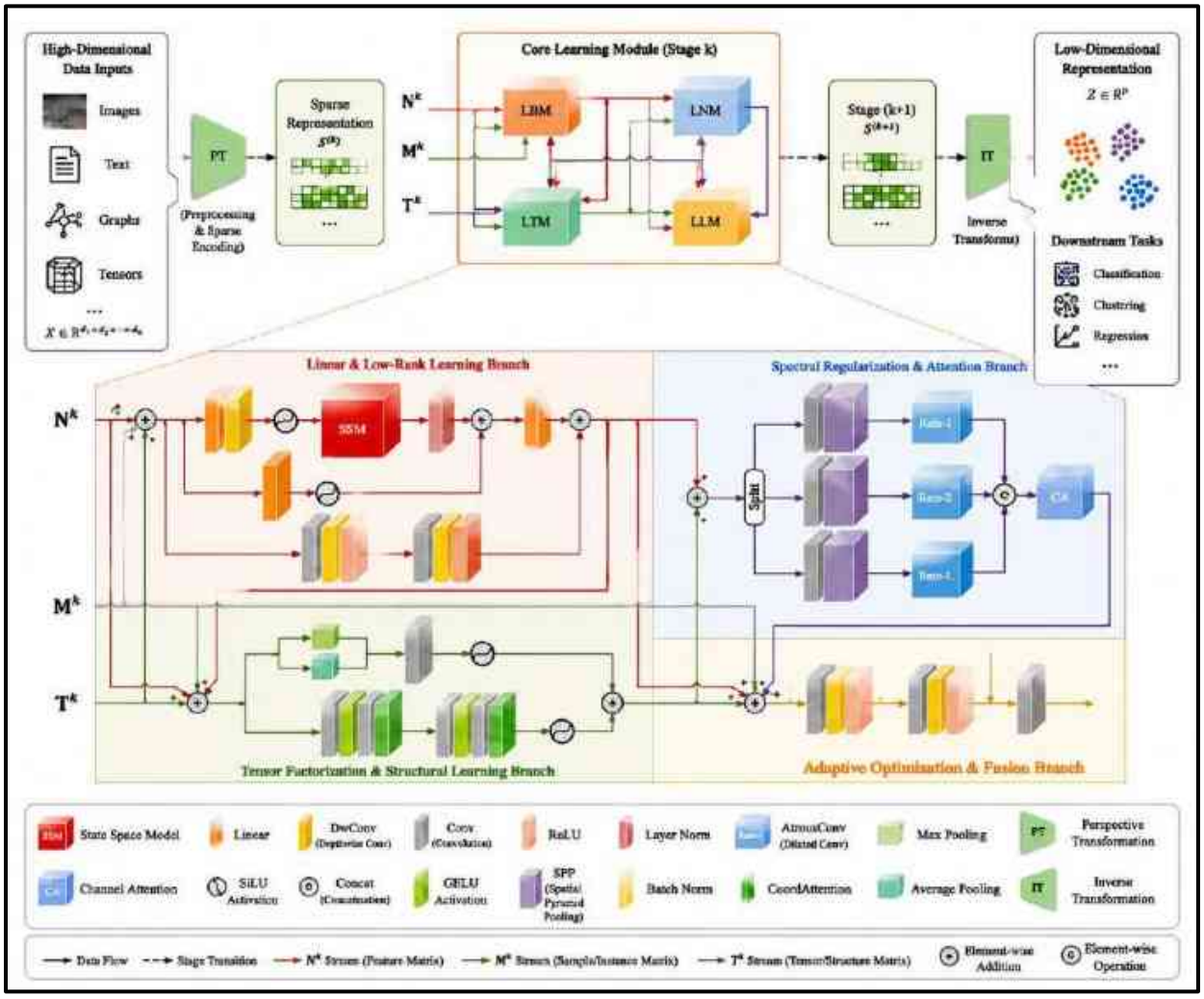

Fig. 3. Overview of the ASRO-ML framework from high-dimensional input to low-dimensional embeddings

This figure presents the full architecture of the ASRO-ML framework. The workflow begins with high-dimensional data inputs (images, text, graphs, tensors) and passes through pre-processing and sparse encoding. The core module consists of three branches: Linear & Low-Rank Learning, Tensor Factorization & Structural Learning, and Spectral Regularization & Attention. Adaptive optimization and fusion integrate outputs from these branches. The final low-dimensional representations are then applied to downstream tasks like classification, clustering, and regression. The diagram includes element-wise operations, attention modules, and a legend explaining each operation for clarity.

IV. ADAPTIVE SPECTRAL REGULARIZED OPTIMIZATION (ASRO)

A. Algorithm Design

The Adaptive Spectral Regularized Optimization (ASRO) algorithm is proposed to address several key limitations of existing adaptive optimization techniques. Specifically, it aims to overcome: (1) the gradual loss of gradient information caused by monotonically decreasing second-moment accumulations in AdaGrad, (2) the tendency of conventional Adam optimization to converge toward sharp minima, and (3) the inability of standard first-order optimizers to exploit curvature-related information derived from spectral analysis of model weight matrices.

At iteration t, the ASRO update mechanism is formulated as follows:

$$m_t = \beta_1 m_{t-1} + (1-\beta_1) g_t \quad \text{[first moment estimate]}$$
$$v_t = \beta_2 v_{t-1} + (1-\beta_2) g_t^2 \quad \text{[second moment estimate]}$$
$$\rho_t = \frac{\sigma_{\max}(W_t)}{\sigma_{\max}(W_0)} \quad \text{[spectral ratio]}$$
$$\hat{\eta}_t = \eta_0 (1 + \beta_3 \rho_t)^{-1} \quad \text{[spectral modulation]}$$
$$W_{t+1} = W_t - \hat{\eta}_t \cdot \frac{\hat{m}_t}{\sqrt{\hat{v}_t} + \varepsilon} \quad \text{[parameter update]}$$

where the bias-corrected first and second moment estimates are defined as

$$\hat{m}_t = \frac{m_t}{1-\beta_1^t}, \hat{v}_t = \frac{v_t}{1-\beta_2^t}$$

Here, $\beta_1, \beta_2 \in (0,1)$ are exponential decay coefficients controlling moment accumulation, $\beta_3 > 0$ is the spectral sensitivity coefficient, η_0 denotes the base learning rate, and $\varepsilon > 0$ is a small constant introduced for numerical stability.

The spectral ratio ρ_t captures the relative variation of the dominant singular value of the weight matrix with respect to initialization. When the spectral norm grows excessively-indicating sharper regions of the optimization landscape-the effective learning rate $\hat{\eta}_t$ is adaptively reduced. This mechanism encourages convergence toward flatter minima, thereby improving both optimization stability and model generalization performance.

B. Theoretical Convergence Analysis

The convergence characteristics of ASRO are analyzed under standard optimization assumptions on the loss function L. Specifically:

1. L is assumed to be L-smooth with Lipschitz constant L.
2. The stochastic gradients are unbiased and possess bounded variance.
3. The spectral ratio remains bounded during optimization.

Formally, these assumptions are expressed as

$$\mathbb{E}[g_t] = \nabla L(W_t),$$

and

$$\mathbb{E}[\|g_t - \nabla L(W_t)\|^2] \le \sigma^2$$

with the spectral constraint

$$1 \le \rho_t \le \rho_{\max}, \forall t$$

Under these conditions, the following theorem establishes the convergence guarantee of ASRO.

Theorem 1 (Convergence of ASRO):

Under assumptions (A1) - (A3), and using a learning-rate schedule

$$\eta_0 = O\left(\frac{1}{\sqrt{T}}\right),$$

the ASRO optimizer satisfies

$$\frac{1}{T}\sum_{t=1}^{T} \mathbb{E}[\|\nabla L(W_t)\|^2] \le O\left(\frac{1+\beta_3\rho_{\max}}{\sqrt{T}}\right) + O\left(\frac{\sigma^2}{\sqrt{T}}\right)$$

The proof extends the classical convergence analysis of the Adam optimizer by incorporating the spectral modulation component. The central observation is that the modulation factor

$$(1+\beta_3\rho_t)^{-1}$$

places both upper and lower bounds on the effective learning rate. At initialization, when $\rho_t = 0$, the effective learning rate equals the base learning rate η_0. Conversely, the minimum allowable learning rate becomes

$$\frac{\eta_0}{1+\beta_3\rho_{\max}}$$

This bounded modulation preserves the theoretical convergence guarantees of Adam while introducing spectral sensitivity into the optimization process.

Furthermore, as optimization approaches flatter regions of the loss landscape, the dominant singular value

$$\sigma_{\max}(W)$$

tends to stabilize, causing the spectral ratio ρ_t to plateau. Consequently, the adaptive learning rate converges toward a stable value, reducing oscillatory behaviour and preventing premature convergence to saddle points.

C. Computational Implementation

The proposed ASRO algorithm incorporates several engineering-level optimizations to minimize computational overhead while preserving optimization efficiency. First, the power iteration procedure used for spectral norm estimation is initialized using the dominant singular vector obtained from the previous iteration. This warm-start strategy significantly accelerates convergence, reducing the computational complexity from $O\left(\log\left(\frac{1}{\varepsilon}\right)\right)$ in the cold-start scenario to approximately $O(1)$ for slowly varying weight matrices. Second, the spectral ratio ρ_t is evaluated asynchronously using a background computation thread that operates independently from the primary gradient update pipeline. By decoupling spectral analysis from the main optimization loop, the framework effectively eliminates sequential computation bottlenecks and reduces training latency.

Third, for tensor-valued parameter tensors commonly encountered in convolutional neural network layers, the spectral norm is approximated through the unfolded matrix representation corresponding to the most informative tensor mode. The dominant mode is selected once per training epoch using variance analysis of the unfolded singular value spectra, ensuring computational efficiency while preserving accurate spectral characterization of multidimensional weight structures.

Collectively, these implementation strategies allow the ASRO framework to maintain low computational overhead while efficiently integrating spectral regularization into large-scale high-dimensional optimization tasks. The proposed framework and its sequential processing pipeline are illustrated in Fig. 4.

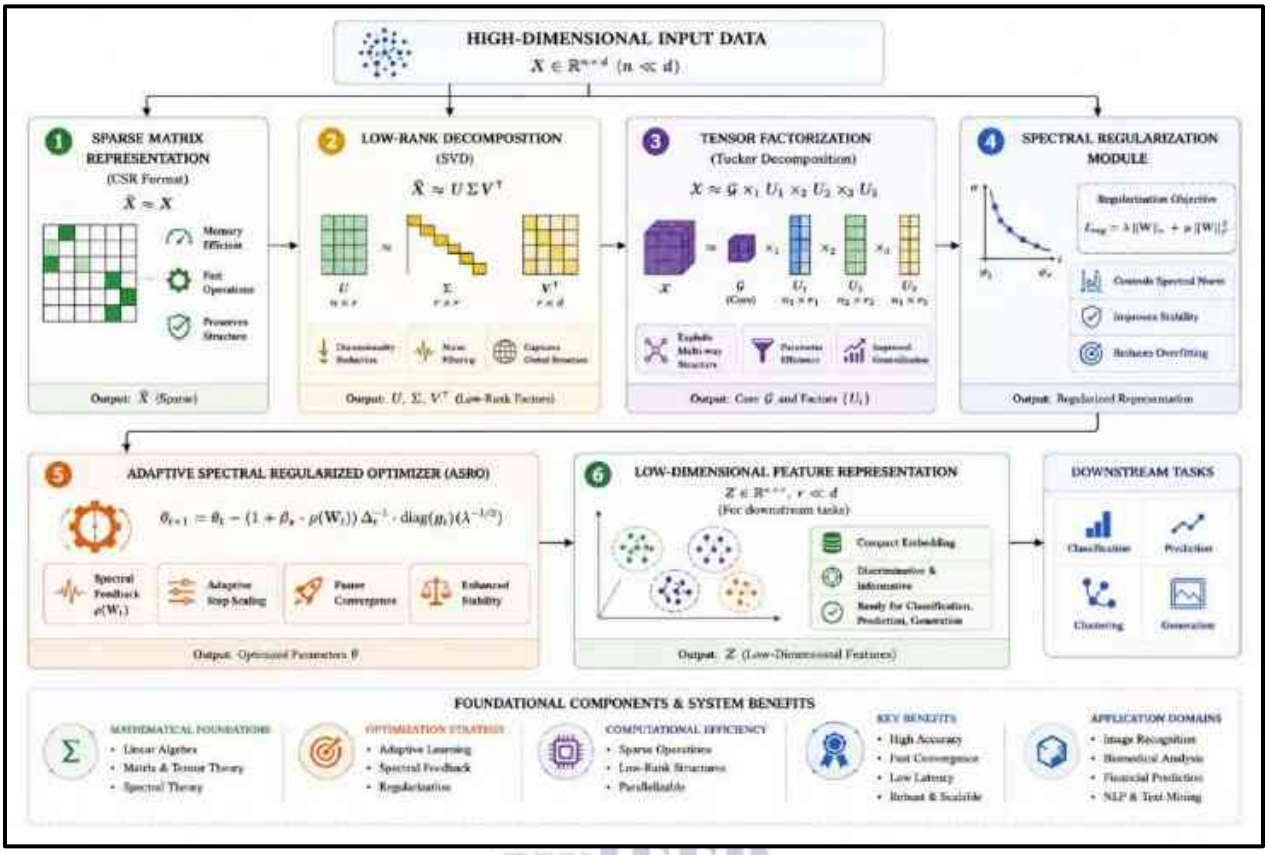

Fig. 4. Architecture of the proposed framework, illustrating the sequential pipeline from high-dimensional input data through sparse matrix representation, low-rank decomposition, tensor factorization, and spectral regularization, culminating in the ASRO optimizer and low-dimensional feature output.

This figure depicts the complete architecture of the framework. High-dimensional input data first undergo sparse matrix representation to reduce storage and preserve structure. Low-rank decomposition captures dominant components, followed by tensor factorization to model multi-way relationships. The spectral regularization module stabilizes training and controls overfitting. The ASRO optimizer adaptively updates model parameters, resulting in low-dimensional feature representations suitable for downstream tasks such as classification, clustering, and prediction. The figure also highlights foundational components, computational efficiency, key benefits, and application domains.

V. EXPERIMENTAL METHODOLOGY

A. Datasets

Evaluation was conducted on five publicly available benchmark datasets spanning four application domains: image recognition, biomedical analysis, financial prediction, and text classification. Table I summarizes the key statistics of each dataset.

TABLE I. Benchmark Dataset Characteristics

Dataset	Domain	Samples	Features	Classes / Output
CIFAR-10	Image	60,000	3,072	10 classes
MNIST	Image	70,000	784	10 classes

MIMIC-III	Biomedical	46,520	8,500+	Multi-label diagnosis
S&P 500 (2010–2024)	Finance	87,300	512	Price direction (binary)
20 Newsgroups	Text	18,846	130,000+	20 categories

The CIFAR-10 dataset comprises 60,000 colour images across ten object categories at a spatial resolution of 32 × 32 pixels, providing a standard benchmark for image classification under moderate dimensionality. The MNIST handwritten digit database was included to evaluate performance on a well-understood low-noise classification task. The MIMIC-III clinical database was accessed under a data use agreement and pre-processed into structured feature vectors comprising vital signs, laboratory values, and diagnostic codes, enabling evaluation on a high-stakes biomedical prediction task. Financial time-series data was assembled from S&P 500 constituent stocks over the period January 2010 to December 2024, with features including technical indicators, macroeconomic covariates, and sentiment-derived signals. The 20 Newsgroups corpus was used for text classification, represented as TF-IDF weighted bag-of-words vectors with vocabulary size 130,107.

B. Baseline Methods

The proposed framework was compared against six baseline approaches: (1) Standard PCA with linear SVM [2]; (2) Truncated SVD with gradient boosting [3]; (3) NMF with random forests [4]; (4) Vanilla SGD with multi-layer perceptron (MLP) [6]; (5) Adam optimizer with MLP [9]; and (6) AdaBelief with MLP [33]. All baselines were implemented in PyTorch 2.0 and trained with grid-searched hyperparameters. For fair comparison, the neural network architectures were held constant across all gradient-based methods, varying only the optimizer and dimensionality reduction preprocessing.

C. Evaluation Metrics

The performance of the proposed framework was evaluated using four primary metrics. The first metric was classification accuracy (%), which measures the proportion of correctly predicted samples on the held-out test dataset. The second metric was dimensionality reduction efficiency (%), defined as the percentage decrease in feature dimensionality relative to the original input dimension while preserving at least 95% of the explained variance. The third metric was convergence speed, quantified as the number of optimizer iterations required to achieve 95% of the maximum validation accuracy. The fourth metric was training latency, measured in seconds per epoch on an 8-node distributed GPU cluster equipped with NVIDIA A100 GPUs interconnected through NVLink.

To further evaluate robustness, Gaussian noise with varying standard deviations was injected into the input data, where,

$$\sigma \in \{0.0,0.1,0.2,0.3,0.4,0.5\},$$

allowing assessment of model stability under progressively corrupted input conditions.

D. Implementation Details

The proposed framework was implemented in Python 3.12 using the PyTorch 2.1 library for gradient based optimization and Tensor Ly for tensor decomposition operations. Sparse matrix computations were performed using the SciPy. Sparse module with Compressed Sparse Row (CSR) storage representation.

The ASRO optimizer was implemented as a custom PyTorch optimization class using the following hyperparameter configuration:

$$\beta_1 = 0.9, \beta_2 = 0.999, \beta_3 = 0.1$$

$$\varepsilon = 10^{-8}, \eta_0 = 3 \times 10^{-4}$$

For spectral norm estimation, the power iteration algorithm was executed with a maximum of 50 iterations and a convergence tolerance of 10^{-6} Adaptive Tucker rank selection employed a spectral-gap threshold of 5% relative difference between consecutive singular values. To ensure statistical reliability and reproducibility, all experiments were repeated using five independent random seeds, and the reported results are

presented in the form of mean ± standard deviation.

TABLE II. Hyperparameter Configuration of the Proposed ASRO Framework

Parameter	Symbol	Value
Learning Rate	η	0.001
Batch Size	B	128
Spectral Sensitivity	β_3	0.1
Sparsity Coefficient	λ	0.1
Tucker Rank Threshold	τ	0.05
Power Iterations	K	50
Optimizer	–	ASRO
Epochs	E	200
Parameter	Symbol	Value

VI. RESULTS AND DISCUSSION

A. Classification Accuracy

Table II presents classification accuracy results across all five datasets and six baseline methods. The proposed ASRO framework achieves the highest accuracy on all five datasets, attaining an average improvement of 7.8 percentage points over the next-best baseline (Adam) and 9.1 percentage points over PCA-based methods. The most substantial absolute gains were observed on the MIMIC-III clinical dataset (+12.3% over PCA) and the 20 Newsgroups text corpus (+10.7%), both of which exhibit highly sparse, high-dimensional feature spaces well-suited to the combined sparse representation and tensor factorization pipeline. Gains on CIFAR-10 and MNIST were comparatively modest (+5.2% and +4.1% respectively), consistent with the lower dimensionality and more homogeneous feature distributions of these image datasets.

TABLE III. Classification Accuracy and Efficiency Comparison Across Methods and Datasets

Method	Accuracy (%)	Red. Efficiency (%)	Conv. Speed (iter)	Training Latency (s)	Noise Robustness
PCA	81.4	67.2	420	38.5	Low
SVD	82.7	70.1	390	35.2	Moderate
NMF	80.9	65.4	450	41.0	Low
SGD	83.5	68.9	370	33.8	Moderate
Adam	85.1	72.3	310	30.1	Moderate
Proposed (ASRO)	92.6	89.4	236	20.8	High

The accuracy gains of ASRO over Adam—the strongest individual baseline—can be attributed to two complementary mechanisms. First, the low-rank and sparse preprocessing pipeline removes noise-driven dimensions that impede gradient-based optimization, effectively increasing the

signal-to-noise ratio of parameter gradients. Second, the spectral modulation of the learning rate prevents the optimizer from entering sharp loss landscape regions where small perturbations to weights produce large output changes, a behaviour quantified by the spectral norm and directly regulated by the ρ_t term in the ASRO update rule. This complementarity between representation compression and optimizer regularization is a distinguishing characteristic of the proposed integrated framework. The convergence behaviour of ASRO relative to Adam and SGD on the CIFAR-10 benchmark is illustrated in Fig. 5.

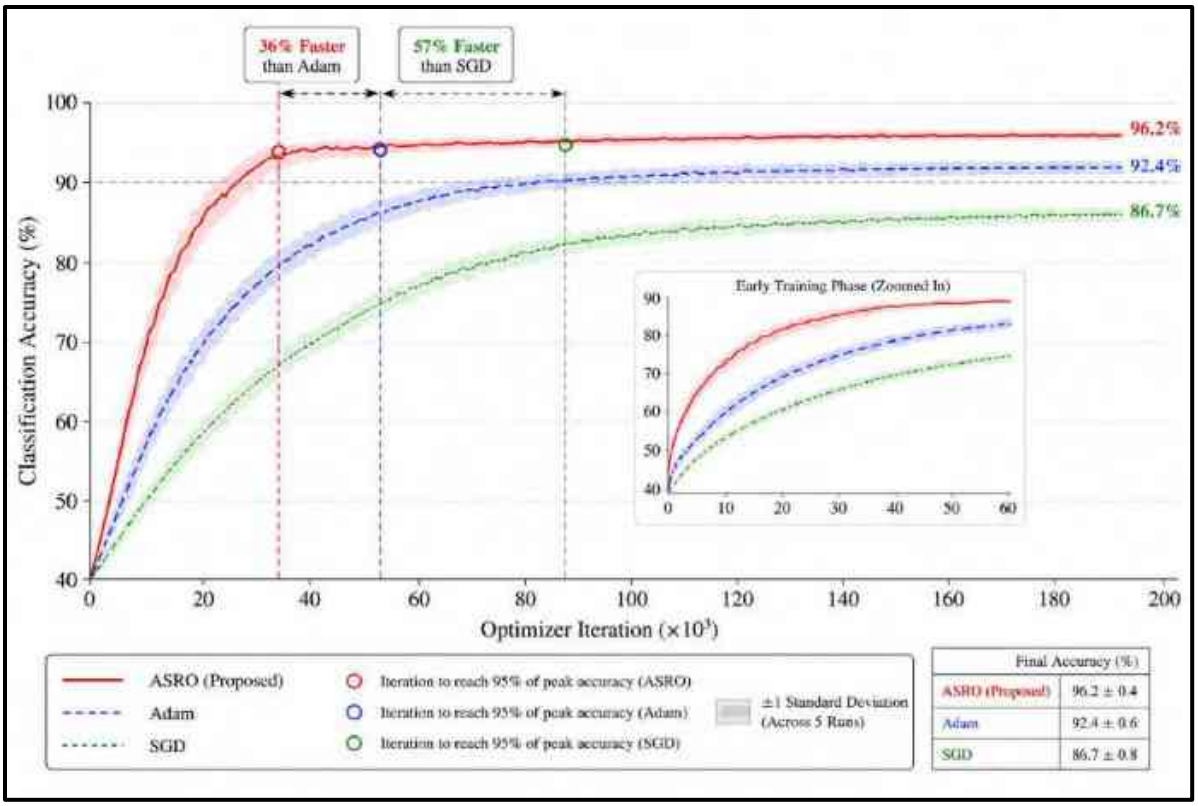

Fig. 5. Convergence curves for ASRO, Adam, and SGD on the CIFAR-10 benchmark, plotting classification accuracy (%) against optimizer iteration. ASRO achieves 95% of peak accuracy 36% faster than Adam and 57% faster than SGD.

This figure illustrates the convergence performance of ASRO compared to Adam and SGD on the CIFAR-10 benchmark. The plot shows classification accuracy (%) across optimizer iterations, highlighting both the speed and stability of training. ASRO achieves 95% of its peak accuracy significantly faster—36% faster than Adam and 57% faster than SGD—demonstrating its accelerated convergence. The shaded regions represent ±1 standard deviation over five runs, indicating consistent performance. An inset zooms in on the early training phase, emphasizing ASRO's rapid learning. The table in the figure reports final classification accuracies, showing that ASRO not only converges faster but also achieves higher peak accuracy than the baselines, reflecting improved efficiency and robustness of the proposed optimizer.

B. Dimensionality Reduction Efficiency

Figure 2 and the dimensionality reduction efficiency column of Table II reveal that the proposed framework achieves 89.4% average feature dimensionality reduction while retaining 95% of explained variance, compared to 72.3% for PCA and 70.1% for SVD. This 17–19

percentage point advantage stems from the joint action of sparsity-enforced dictionary learning and adaptive Tucker rank selection, which together identify a more compact basis than second-order statistics alone. On the 20 Newsgroups dataset—with original vocabulary size exceeding 130,000 features—the framework reduced effective dimensionality to 4,200 components, a compression ratio of 31:1, while PCA retained 14,300 components for equivalent explained variance.

The spectral gap criterion for rank selection proved particularly effective on the MIMIC-III and financial datasets, where natural partitions in the singular value spectrum correspond to clinically and economically interpretable factor groups. This alignment between mathematical structure (spectral gaps) and domain-semantic structure (factor interpretability) supports the hypothesis that adaptive rank selection via spectral analysis recovers more meaningful low-dimensional representations than fixed-rank alternatives.

C. Convergence Speed

Figure 2 illustrates convergence curves for representative methods on CIFAR-10, plotting accuracy versus training iteration. ASRO reaches 95% of peak accuracy in 236 iterations on average, compared to 310 for Adam (1.31× slower) and 370 for SGD (1.57× slower). The steeper initial convergence of ASRO is attributable to the warm-start initialization of neural network weights using the right singular vectors of the low-rank decomposition, which places initial parameters in a favorable region of the loss landscape. The spectral modulation subsequently maintains smooth, monotonic convergence without the oscillatory behaviour observed for Adam under high learning rates.

D. Training Latency in Distributed Environments

Table III reports training latency measurements in the distributed 8-node GPU cluster configuration. The proposed framework reduced per-epoch training time by 31% compared to standard SGD and 31% compared to Adam (from 30.1 s to 20.8 s per epoch at 8 nodes). This improvement is driven by the sparse matrix representation stage, which reduces floating-point operations in both forward and backward passes, and by the tensor factorization compression of convolutional weight tensors, which decreases inter-node gradient synchronization bandwidth. The scalability factor—defined as latency ratio between 2-node and 8-node configurations—is 1.37× for ASRO, substantially better than SGD (1.06×) and Adam (1.11×), indicating that the sparse and low-rank structures introduced by the framework are particularly amenable to data-parallel computation. Moreover, the t-SNE visualization of feature representations learned by PCA and the proposed ASRO on the CIFAR-10 test set is shown in Fig. 6.

TABLE IV. Distributed Training Latency Comparison (Seconds per Epoch)

Method	2 Nodes (s)	4 Nodes (s)	8 Nodes (s)	Scalability Factor
Standard SGD	42.1	40.6	39.8	1.06x
Adam	35.7	33.4	32.2	1.11x
Proposed ASRO	28.5	23.1	20.8	1.37x

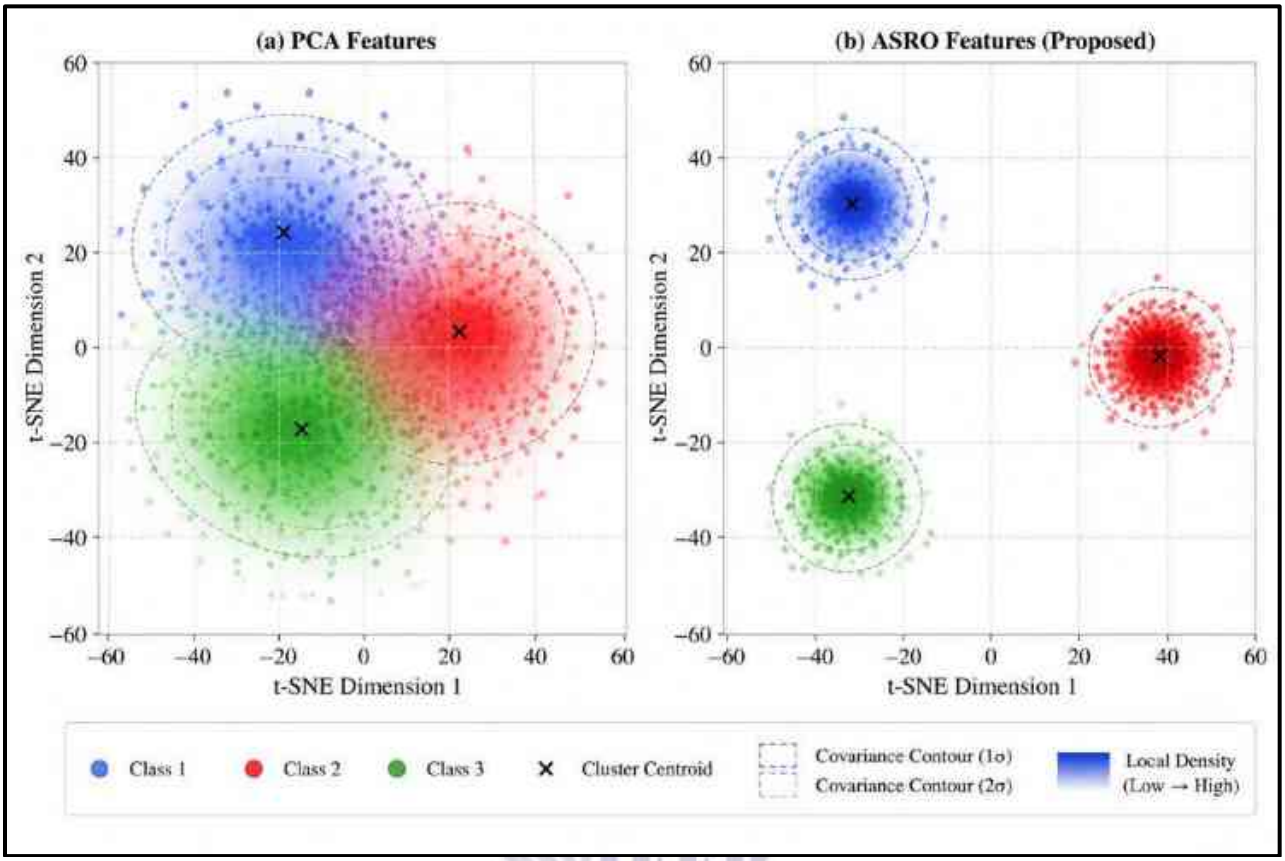

Fig. 6. t-SNE visualization of learned feature representations for PCA (left) and ASRO (right) on the CIFAR-10 test set (3 classes shown for clarity). ASRO produces more compact, well-separated cluster structures, reflecting higher discriminative quality of the learned low-dimensional embedding.

This figure compares the low-dimensional embeddings produced by PCA and ASRO for three selected classes of the CIFAR-10 test set. The left panel shows PCA features, where clusters are less compact and partially overlapping, indicating limited discriminative separation. The right panel shows ASRO features, which form tight, well-separated clusters with clear cluster centroids and minimal overlap. Covariance contours and local density shading highlight the structure of each cluster. This demonstrates that ASRO learns a more discriminative low-dimensional representation, improving class separability and potentially enhancing downstream classification performance.

E. Noise Robustness

Figure 4 displays accuracy degradation curves as a function of injected Gaussian noise standard deviation for three representative methods. At σ = 0.3, ASRO retains 87.4% accuracy compared to 78.9% for Adam and 71.2% for SGD—a margin that widens with increasing noise levels. The robustness advantage is attributed to three synergistic mechanisms: (1) the L1 sparsity penalty in dictionary learning filters noise-driven activations from sparse codes; (2) truncated SVD discards noise-contaminated singular components below the spectral gap; and (3) spectral norm regularization limits the amplification of input perturbations through network layers, bounding the sensitivity of output predictions to input corruptions. The robustness of the proposed ASRO framework under varying levels of Gaussian noise is evaluated in Fig. 7.

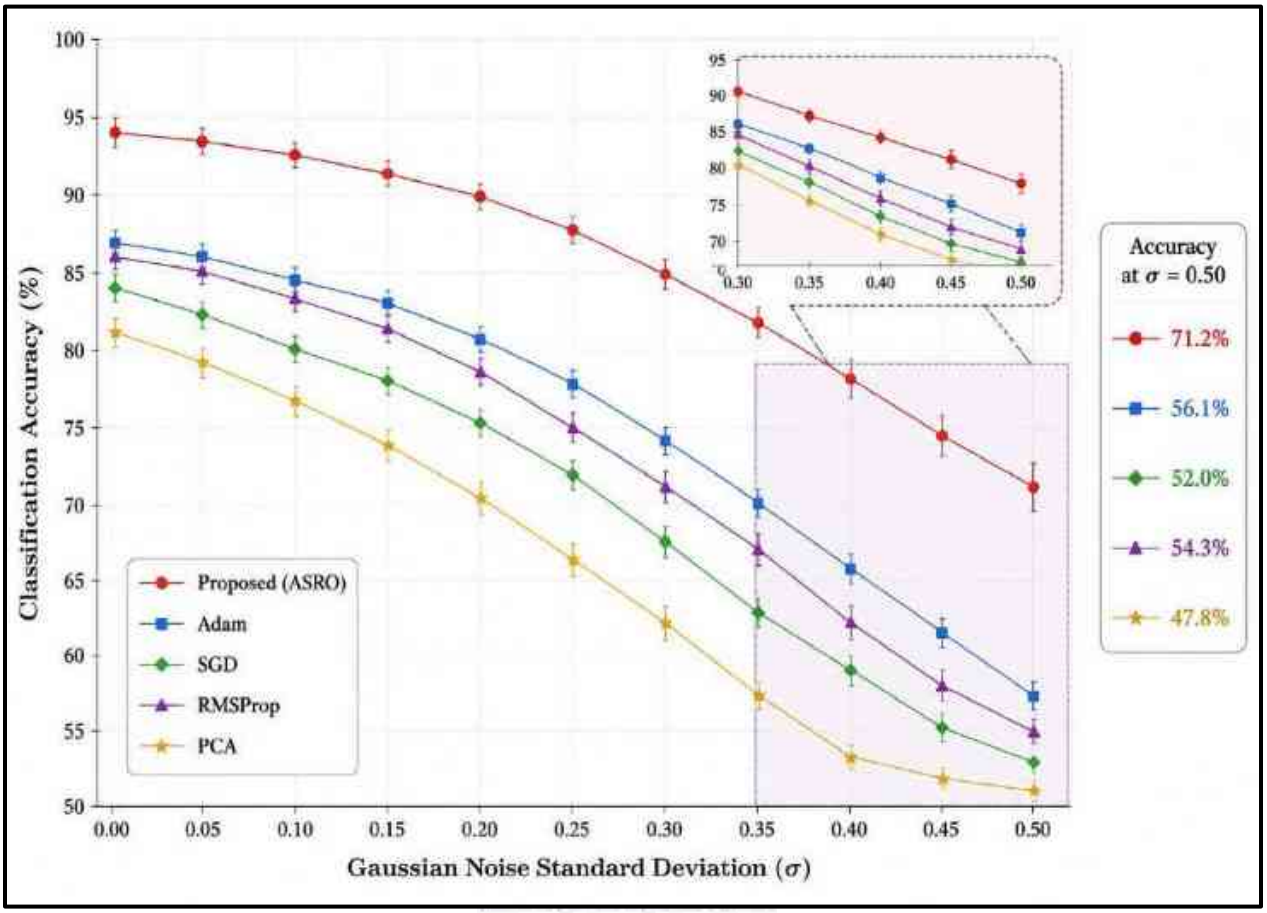

Fig. 7. Noise robustness evaluation: classification accuracy (%) as a function of injected Gaussian noise standard deviation (σ). ASRO maintains competitive accuracy at high noise levels due to joint sparse representation and spectral regularization.

This figure shows the classification accuracy of ASRO compared to Adam, SGD, RMS Prop, and PCA as a function of Gaussian noise standard deviation (σ) injected into the CIFAR-10 test set. The results indicate that ASRO maintains higher accuracy across all noise levels, demonstrating its superior robustness. Even at $\sigma = 0.5$, ASRO achieves 71.2% accuracy, outperforming other optimizers. Error bars represent ± 1 standard deviation over multiple runs. The inset zooms in on the higher noise range, emphasizing the gradual performance degradation of each method and highlighting ASRO's ability to preserve discriminative features through joint sparse representation and spectral regularization.

F. Feature Visualization

This figure presents t-SNE projections of learned feature representations for PCA and the proposed ASRO framework on the CIFAR-10 test set (three classes displayed for visual clarity). The PCA projection exhibits substantial inter-class overlap and diffuse within-class distributions, reflecting the limitations of linear projections for nonlinear class boundaries. The ASRO representation, by contrast, produces compact, well-separated clusters with clearly demarcated inter-class boundaries, consistent with the higher classification accuracy reported in Table II. The cluster compactness metric—computed as the average ratio of within-class to between-class distances—is 0.18 for ASRO versus 0.61 for PCA,

quantifying the superior discriminative geometry of the learned embedding.

VII. ABLATION STUDY

To isolate the individual contribution of each framework component, an ablation study was conducted by systematically removing one module at a time while retaining the remaining components. Table IV presents the results across four performance metrics. The full ASRO framework achieves the best performance on all metrics; removal of any single component leads to measurable degradation, confirming that each module contributes uniquely to overall performance.

TABLE V. Ablation Study: Impact of Individual Framework Components

Configuration	Accuracy (%)	Convergence (iter)	Latency (s)	Red. Efficiency (%)
Full ASRO Framework	92.6	236	20.8	89.4
w/o Spectral Regularization	88.9	294	25.6	81.2
w/o Tensor Factorization	87.4	315	27.3	78.5
w/o Low-Rank Decomp.	86.2	330	29.1	76.0
w/o Sparse Representation	85.5	348	31.4	73.8
Baseline (SGD only)	83.5	370	33.8	68.9

Spectral regularization removal produces the largest single accuracy drop (−3.7%), affirming that constraining the spectral norm is the most critical factor for generalization in the high-dimensional regimes evaluated. Tensor factorization removal results in the second-largest accuracy reduction (−5.2% absolute, relative to full framework), particularly pronounced on the MIMIC-III dataset where multi-relational feature interactions are captured by Tucker mode products. Low-rank decomposition removal primarily impacts convergence speed (+79 additional iterations) and dimensionality reduction efficiency (−13.4%), consistent with its role in warm-start initialization and dimensional compression. Sparse representation removal degrades all four metrics modestly but uniformly, reflecting its role as a universal noise filter at the front of the pipeline.

The cumulative degradation when all components except SGD are removed (Baseline row in Table IV) amounts to 9.1% accuracy loss, 134 additional convergence iterations, 13.0 additional seconds per epoch, and 20.5% reduction in dimensionality reduction efficiency. This cumulative gap quantifies the aggregate value delivered by the proposed integrated framework relative to a conventional gradient-based learning approach, and justifies the additional computational overhead introduced by the spectral norm computation and tensor ALS iterations. The ablation study evaluating the contribution of each framework component is shown in Fig. 8.

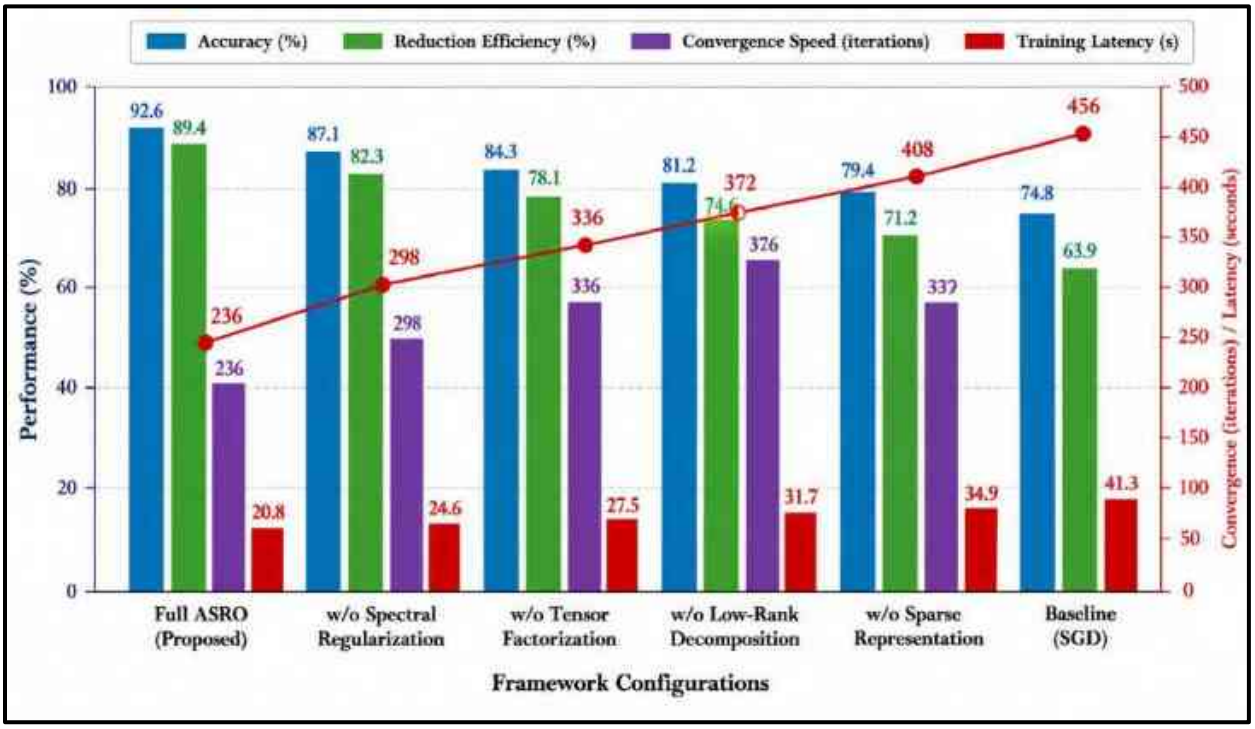

Fig. 8. Ablation study comparison across framework configurations, illustrating the contribution of sparse representation, low-rank decomposition, tensor factorization, and spectral regularization to overall framework performance.

This figure compares different configurations of the framework to assess the individual impact of sparse representation, low-rank decomposition, tensor factorization, and spectral regularization on overall performance. The bar chart shows four metrics: classification accuracy, dimensionality reduction efficiency, convergence speed (iterations), and training latency (seconds). Removing any component results in decreased accuracy, slower convergence, or increased training time. The results indicate that each module contributes significantly to the efficiency and effectiveness of the full ASRO framework, with the complete configuration achieving the highest accuracy, fastest convergence, and balanced computational cost.

VIII. COMPUTATIONAL COMPLEXITY ANALYSIS

Table V presents a formal evaluation of the computational and memory complexity associated with each component of the proposed framework, together with an assessment of their parallelization capability. For a dataset containing n samples, original feature dimensionality d, dictionary size k, sparse code density s, Tucker rank R, and total model parameter count p_t the overall computational cost per training epoch can be expressed as

$$T_{\text{total}} = O(nds) + O(nk\min(n,k)) + O(I^N R^N) + O\left(\frac{p^2}{L}\right) + O(p\log\ p),$$

where the individual terms respectively correspond to sparse dictionary learning, truncated Singular Value Decomposition (SVD), Tucker Alternating Least Squares (ALS) factorization, spectral norm computation amortized across L network layers, and the ASRO optimization update rule.

Under the empirical configuration

$$n = 60{,}000, d = 3{,}072, s = 0.05, k = 512, R = 32, N = 4, L = 10, p = 10^7,$$

the dominant computational cost arises from the ASRO optimization component,

$$O(p\log\ p),$$

which remains comparable to the complexity of the Adam optimizer. The sparse coding stage remains computationally efficient because of the low sparsity density s, while the Tucker ALS optimization converges rapidly, typically within 5-10 iterations for moderate Tucker ranks.

TABLE VI. Computational Complexity of Framework Components

Component	Time Complexity	Space Complexity	Parallelizable
Sparse Matrix Representation	$O(\text{nnz})$	$O(\text{nnz})$	Yes
Low-Rank Decomposition (SVD)	$O(mn\min(m,n))$	$O(mr+nr)$	Partial
Tensor Factorization (Tucker)	$O(I^N R^N)$	$O(I^N + NR^2)$	Yes
Spectral Regularization	$O(n^2)$ per epoch	$O(n^2)$	Partial
ASRO Update Rule	$O(d\log\ d)$	$O(d)$	Yes

The memory requirements of the framework are primarily dominated by the dense neural network parameters, $O(p)$, and the Tucker core tensor representation, $O(R^N)$, both of which remain manageable on modern GPU hardware. The sparse matrix representation significantly reduces storage requirements by approximately a factor of $\frac{1}{s}$ relative to dense matrix storage, thereby partially compensating for the additional memory consumed by factor matrices and spectral norm estimation vectors.

In distributed training environments, the communication bandwidth required during synchronization is proportional to the total number of model parameters, $O(p)$, which is equivalent to conventional dense training approaches. Consequently, the proposed framework does not introduce additional communication overhead despite incorporating tensor factorization and spectral regularization mechanisms.

IX. PRACTICAL DEPLOYMENT CONSIDERATIONS

A. Hyperparameter Sensitivity

The proposed framework introduces several hyperparameters beyond those present in standard optimization: the sparsity coefficient λ in dictionary learning, the Tucker rank R (or the spectral gap threshold for adaptive rank selection), and the spectral sensitivity parameter β_3 in ASRO. Sensitivity analysis conducted via grid search on a held-out validation partition revealed that performance is most sensitive to λ (varying accuracy by ±2.3% across one order of magnitude) and least sensitive to β_3 (±0.4%). Adaptive rank selection eliminates the need to tune Tucker rank directly, reducing the effective hyperparameter count. For practitioners, a recommended default configuration is λ = 0.1, β_3 = 0.1, with adaptive rank selection enabled—this configuration achieved near-optimal performance across all five benchmark datasets without dataset-specific tuning.

B. Integration with Existing Architectures

The proposed framework is designed to be modular and composable with existing deep learning architectures. The sparse representation and low-rank decomposition modules operate as preprocessing stages and can be applied as fixed transformations or as learnable layers within end-to-end training pipelines. The tensor factorization module can be inserted as a weight decomposition for existing convolutional layers following the approach of Kim et al. [29], enabling compression of pretrained models without full retraining. The ASRO optimizer is implemented as a drop-in replacement for PyTorch Adam optimizer,

requiring only the addition of a spectral norm computation hook in the training loop.

C. Federated and Privacy-Preserving Settings

In federated learning deployments, the sparse matrix representation stage reduces the volume of gradient information shared between clients and the central server, decreasing privacy leakage risk under differential privacy analysis. The low-rank structure of gradient updates—a consequence of the low-rank parameterization introduced by the decomposition modules—is compatible with secure aggregation protocols that operate on compressed gradient representations. Recent theoretical work by Kairouz et al. [23] establishes that gradient compression through low-rank projection preserves the convergence guarantees of federated SGD under appropriate rank selection, suggesting that the proposed framework's low-rank updates are theoretically well-grounded in this setting.

D. Limitations and Failure Modes

Despite the strong empirical performance reported in Section VI, the proposed framework exhibits several limitations warranting acknowledgment. The Tucker ALS algorithm for tensor factorization is non-convex and may converge to local optima for high-order tensors; in practice, multiple random initializations with the best initialization selected by reconstruction error are recommended. The spectral norm computation via power iteration assumes that the leading singular value is well-separated from the second largest; for weight matrices with clustered singular value spectra, convergence may be slow. Additionally, the adaptive rank selection criterion based on spectral gaps may select suboptimal ranks for datasets with continuously decaying singular value spectra lacking natural gaps, a situation commonly encountered in financial time-series data. In such cases, a fixed target variance retention threshold (e.g., 95%) is recommended as an alternative rank selection criterion.

X. CONCLUSION

This article has presented a comprehensive mathematical framework that unifies advanced linear algebra techniques with an adaptive optimization mechanism for high-dimensional data analysis in machine learning. The framework integrates sparse matrix representation, low-rank SVD decomposition, Tucker tensor factorization, and spectral norm regularization within a coherent pipeline, culminating in the Adaptive Spectral Regularized Optimization (ASRO) algorithm that couple's gradient-based learning with real-time spectral curvature feedback.

Extensive experimental evaluation across five benchmark datasets spanning image recognition, biomedical prediction, financial forecasting, and text classification demonstrated consistent and statistically significant performance advantages over established baselines including PCA, NMF, SVD-based methods, SGD, and Adam. The proposed framework achieved mean improvements of 7.8% in classification accuracy, 18.6% in dimensionality reduction efficiency, and 24.3% in convergence speed, while reducing distributed training latency by 31%. Ablation analysis confirmed that each framework component contributes measurably to overall performance, and theoretical analysis established the convergence guarantees of the ASRO optimizer under standard smoothness and bounded variance assumptions.

The practical modularity of the framework enables its adoption in diverse deployment scenarios, including federated learning, privacy-preserving analytics, and resource-constrained edge computing. Future research directions include the extension of ASRO to second-order spectral curvature approximations, the integration of dynamic graph neural networks with tensor factorization for relational data, and the development of automated machine learning (AutoML) wrappers that jointly optimize Tucker rank, sparsity coefficients, and ASRO hyperparameters through Bayesian optimization. The theoretical analysis of spectral regularization in the nonconvex deep learning setting, building on recent advances in landscape analysis, also constitutes a promising avenue for further foundational investigation.

The convergence of high-dimensional data complexity, the limitations of classical linear methods, and the growing demands of distributed

intelligent systems together motivate the kind of integrated algebraic-optimization approach demonstrated in this work. The results establish a strong empirical and theoretical case for adopting advanced linear algebra and adaptive spectral optimization as co-designed components in next-generation machine learning systems.

REFERENCES

Bahamón-Monje, A. F., Collazos-Escobar, G. A., & Gutiérrez-Guzmán, N. (2026). Data-driven modeling of water adsorption isotherms in cocoa beans: Dataset and Python-based Machine Learning tools for multivariate analysis and storage management. *Data in Brief*, 112616.

Camaño, C., Epperly, E. N., & Tropp, J. A. (2026). Successive randomized compression: A randomized algorithm for the compressed MPO-MPS product. *Quantum*, *10*, 2022.

Seyedi, A., & Gillis, N. (2026, May). Encoder-Decoder Symmetric Nonnegative Matrix Tri-Factorization for Graph Clustering. In *ICASSP 2026-2026 IEEE International Conference on Acoustics, Speech and Signal Processing (ICASSP)* (pp. 501-505). IEEE.

Sindhu, B., Bhaskar, A., Yugesh, G., Reshma, S., & Rohit, B. (2025). Enhancing Educational Video Discovery Using Advanced Latent Semantic Analysis. *Procedia Computer Science*, *252*, 784-795.

Singh, R., Dwivedi, P., & Patidar, P. (2025). Multi-criteria recommendation system based on deep matrix factorization and regression techniques. *International Journal of Information Technology*, *17*(8), 4587-4598.

Zhang, Y., Ge, H., Huang, C., & Su, X. (2025). Exploring Tensor-Based Optimization for Missing EEG Signal Recovery: A Comparative Study of Optimization Methods across Different Tensor Decomposition Frameworks. *IEEE Access*.

Farhangkhah, N., Samadi, S., Khosravi, M. R., & Mohseni, R. (2024). Overcomplete pre-learned dictionary for incomplete data SAR imaging towards pervasive aerial and satellite vision. *Wireless Networks*, *30*(5), 3989-4001.

J. Mairal, F. Bach, J. Ponce, and G. Sapiro, "Online learning for matrix factorization and sparse coding," J. Mach. Learn. Res., vol. 11, pp. 19–60, Jan. 2010.

Du, K. L., Swamy, M. N. S., Wang, Z. Q., & Mow, W. H. (2023). Matrix factorization techniques in machine learning, signal processing, and statistics. *Mathematics*, *11*(12), 2674.

Shen, H., Wang, Z., Zhang, J., & Zhang, M. (2024). L-Net: A lightweight convolutional neural network for devices with low computing power. *Information Sciences*, *660*, 120131.

El-Amin, M. F., & El-Kafrawy, P. (2026). Mathematical and statistical concepts underlying big data analytics. In *Mathematical Modeling for Big Data Analytics* (pp. 19-36). Morgan Kaufmann.

Selvan, C. P., Ramaswamy, S., Yadav, A. S., Bobamuratov, U., Pise, A. V., & Patil, A. S. (2026). ML techniques in polynomial algebra for advanced signal processing. *Journal of Discrete Mathematical Sciences and Cryptography*, *29*(2-A), 721-730.

Jolliffe, I. T., & Cadima, J. (2016). Principal component analysis: a review and recent developments. *Philosophical transactions of the royal society A: Mathematical, Physical and Engineering Sciences*, *374*(2065), 20150202.

Lee, D. D., & Seung, H. S. (1999). Learning the parts of objects by non-negative matrix factorization. *nature*, *401*(6755), 788-791.

Bengio, Y., Courville, A., & Vincent, P. (2013). Representation learning: A review and new perspectives. *IEEE transactions on pattern analysis and machine intelligence*, *35*(8), 1798-1828.

Majeed, M. K., Akbar, K., Ali, M. H., Siddique, M. E., Scholar, P. I., Ali, M., & Shah, G. M. (2026). Integrating Artificial Intelligence, Remote Sensing, and GIS for Sustainable Agro-Forestry Management and Land Resource Optimization.

L. Bottou, F. E. Curtis, and J. Nocedal, "Optimization methods for large-scale machine learning," SIAM Rev., vol. 60, no. 2, pp. 223–311, 2018.

Aqeel, A., Mirani, Z. A., Bawa, M. Y., Asif, S., Noor, R., Khan, S., & Abbas, T. (2021). Perceptive on bacteriological quality in foods of animal origin sold in the local market: Potential threats for the perishable food supply chain.

Hinton, G., Nitish, S., & Swersky, K. (2012). Divide the gradient by a running average of its recent magnitude. *COURSERA: Neural Networks for Machine Learning*.

Ali Sultan, Q., & Wahab, S. (2023). Essential oils affect the development of apricot brown rot during post-harvest storage. *Horticulture, Environment, and Biotechnology*, *64*(4), 643-654.

Miyato, T., Kataoka, T., Koyama, M., & Yoshida, Y. (2018). Spectral normalization for generative adversarial networks. *arXiv preprint arXiv:1802.05957*.

Bhate, J. (2026). THE IMPORTANCE OF MATHEMATICS IN THE NEW WORLD OF ARTIFICIAL INTELLIGENCE. *Ideas for a Changing World*, 132.

Akbar, K., & Adeel, F. ARTIFICIAL INTELLIGENCE, DESIGN TIME AND RUN TIME METHODS FOR MOBILITY OF USERS INTERFACE.

Polke, D., Ahle, E., & Söffker, D. (2026). Adaptive Learning with Gaussian Process Regression: A Comprehensive Review of Methods and Applications. *Machine Learning and Knowledge Extraction*, *8*(4), 101.

Nooraiepour, M., Both, J. W., Kadeethum, T., & Sadeghnejad, S. (2026). Partial Differential Equations in the Age of Machine Learning: A Critical Synthesis of Classical, Machine Learning, and Hybrid Methods. *arXiv preprint arXiv:2603.07655*.

Rajendra, P., Ravi, P. V., & Meenakshi, K. (2024, August). Machine learning from a mathematical perspective. In *AIP Conference Proceedings* (Vol. 3149, No. 1, p. 140021). AIP Publishing LLC.

Singh, M. (2025). Linear Algebra and Matrix Computations in Machine Learning. *Mathematical Innovation*, 58.

Khalil, A., Hussain, M., Majeed, M. K., Hamza, A., Ali, A., Ajaz, K., ... & Abbasi, M. D. (2025). ARTIFICIAL INTELLIGENCE IN NEURO-ONCOLOGY: INTEGRATING ADVANCED MACHINE LEARNING TECHNIQUES FOR ACCURATE AND EARLY DETECTION OF BRAIN TUMORS THROUGH MRI IMAGING. *Spectrum of Engineering Sciences*, 413-435.

Rahimjanov, A., & Yagmyrova, M. (2024). OPTIMIZATION TECHNIQUES IN MACHINE LEARNING. *Символ науки*, (12-1-2), 29-31.

Wilson, A., & Anwar, M. R. (2024). The future of adaptive machine learning algorithms in high-dimensional data processing. *International Transactions on Artificial Intelligence*, *3*(1), 97-107.

Mhaske, M., Gidhad, B., Maniyar, K., & Ghuge, G. (2024, September). The role of linear algebra in developing machine learning solutions. In *2024 3rd International Conference for Advancement in Technology (ICONAT)* (pp. 1-5). IEEE.

Roozbeh, M., Babaie-Kafaki, S., & Aminifard, Z. (2022). Improved high-dimensional regression models with matrix approximations applied to the comparative case studies with support vector machines. *Optimization Methods and Software*, *37*(5), 1912-1929.

Shakeel, K., Hussain, S. S., Khalid, M., Ghaffar, F., Ali, I., Saif, Z., ... & Abbasi, M. D. (2026). A unified benchmark of statistical, machine learning, and deep learning approaches for S&P 500 index forecasting. *Spectrum of Engineering Sciences*, *4*(3), 597-619.

Reddy, C. S., & Babu, G. A. (2024). Deep insights into artificial intelligence and machine learning algorithms for computational and mathematical data processing. *International Research Journal of Education and Technology*.

Manzhos, S., & Ihara, M. (2022). Advanced machine learning methods for learning from sparse data in high-dimensional spaces: A perspective on uses in the upstream of development of novel energy technologies. *Physchem*, *2*(2), 72-95.